Bull. Mater. Sci., Vol. 26, No. 1, January 2003, pp. 193–197. © Indian Academy of Sciences.

A study of phase separation in ternary alloys

SASWATA BHATTACHARYYA and T A ABINANDANAN*

Department of Metallurgy, Indian Institute of Science, Bangalore 560 012, India

Abstract. We have studied the evolution of microstructure when a disordered ternary alloy is quenched into a ternary miscibility gap. We have used computer simulations based on multicomponent Cahn–Hilliard (CH) equations for c_A and c_B, the compositions (in mole fraction) of A and B, respectively. In this work, we present our results on the effect of relative interfacial energies on the temporal evolution of morphologies during spinodal phase separation of an alloy with average composition, $c_A = 1/4$, $c_B = 1/4$ and $c_C = 1/2$. Interfacial energies between the 'A' rich, 'B' rich and 'C' rich phases are varied by changing the gradient energy coefficients. The phases associated with a higher interfacial energy are found to be more rounded than those with lower energy. Further, the kinetic paths (i.e. the history of A-rich, B-rich and C-rich regions in the microstructure) are also affected significantly by the relative interfacial energies of the three phases.

Keywords. Ternary systems; Cahn–Hilliard equations; spinodal decomposition.

1. Introduction

Most of the technologically important alloys are multicomponent systems, exhibiting multiple phases in their microstructures. Moreover, one or more of these phases are formed as a result of phase transformations induced during processing. Since performance of these multicomponent alloys depends crucially on the morphology of the phases, a fundamental understanding of the kinetics of phase transformations is important for controlling the microstructures of these multi-phase alloys. With this motivation, we have studied the kinetics of phase separation in a ternary system.

The phase separation dynamics in binary alloys undergoing spinodal decomposition have been extensively studied, both experimentally and theoretically, and most of the earlier investigations were summarized by Hilliard (1970). Ternary phase diagrams for simple model systems were calculated by Meijering (1950, 1951) and Kikuchi *et al* (1977) and Kikuchi (1997). The thermodynamic stability and the early stages of spinodal decomposition kinetics for ternary systems were analysed by de Fontaine (1972, 1973) and Morral and Cahn (1971). Hoyt (1989) extended Langer's (1971, 1973) theory for binary solutions to the case of ternary alloys and derived nonlinear diffusion equations for the local composition and three independent partial structure functions. More recently, Hoyt (1998) studied coarsening in multiphase, multicomponent systems within the mean field limit.

The nonlinear dynamics of the microstructural evolution during the process of spinodal decomposition in ternary alloys have been studied by Chen (1994) and Eyre (1995). They studied the effect of various alloy compositions on the kinetic paths during phase separation. The interfacial energies between all the coexisting phases were considered to be equal in their study. Since interfacial energies also play a very important role during microstructural evolution, the main objective of our work is to study the effect of relative interfacial energies on the temporal evolution of microstructure during spinodal decomposition of ternary alloys. In §2 of this paper, we briefly describe the model and the technique for solving the diffusion equations. In §3, we describe the microstructures and discuss the effect of interfacial energies on them. In §4 we summarize our studies.

2. Model system

We consider a ternary alloy system consisting of three different atomic species A, B and C. Let $c_i(\mathbf{r}, t)$ for $i = $ A, B, C represent the mole fraction of the ith component of the alloy as a function of position, $\mathbf{r}$ and time, t. Since c_i is a mole fraction, we have the following condition

$$c_A + c_B + c_C = 1. \tag{1}$$

We assume that the free energy (per molecule), $f(c_A, c_B, c_C)$, is given by the regular solution expression

$$\frac{1}{k_B T} f(c_A, c_B, c_C) = \sum_{i \neq j} \chi_{ij} c_i c_j + \sum_i c_i \ln c_i,$$

where χ_{ij} $(= \omega_{ij}/k_B T;\ i, j = $ A, B, C; $i \neq j)$ is the effective interaction energy between the components, i and j, k_B is the Boltzmann's constant and T the absolute temperature. Note that χ_{ij} is inversely proportional to the temperature. Here we consider symmetric A–B–C ternary alloys for our present study, i.e. $\chi_{AB} = \chi_{BC} = \chi_{AC} = \chi$. If $\chi \geq 3$, then

*Author for correspondence

it can be shown that the bulk free energy density has three minima and one maximum; in other words, the system exhibits a ternary miscibility gap. At high temperatures an alloy with a composition of $A_{25}B_{25}C_{50}$, say, is homogeneous and disordered. When such a single phase disordered alloy is quenched to low temperatures ($\chi \geq 3$), the alloy becomes unstable with respect to ternary phase separation.

The Cahn–Hilliard free energy functional, $\mathcal{F}$ (Cahn and Hilliard 1958), for a compositionally inhomogeneous ternary alloy can then be written as

$$\frac{\mathcal{F}}{k_B T} = N_v^* \int_V [f(c_A, c_B, c_C) + K_A^* (\nabla c_A)^2 + K_B^* (\nabla c_B)^2 + K_C^* (\nabla c_C)^2] \mathrm{d}V, \quad (2)$$

where N_v^* is the number of molecules per unit volume (assumed to be a constant), K_A^*, K_B^* and K_C^* are the bare gradient energy coefficients associated with gradients of compositions A, B and C, respectively.

Due to the condition in (1), we need to solve for the evolution of only two of the composition variables, say, c_A and c_B. The non-dimensional forms of the evolution equations are (details can be found in Huang *et al* 1995; Bhattacharyya 2002)

$$\frac{\partial c_A}{\partial t} = M_{AA}\{\nabla^2(\partial f / \partial c_A) - 2K_{AA}\nabla^2 c_A - 2K_{AB}\nabla^2 c_B\} + M_{AB}\{\nabla (\partial f / c_B) - 2K_{AB}\nabla c_A \; 2K_{BB}\nabla c_B\}, \quad (3)$$

$$\frac{\partial c_B}{\partial t} = M_{BA}\{\nabla^2(\partial f / \partial c_A) - 2K_{AA}\nabla^2 c_A - 2K_{AB}\nabla^2 c_B\} + M_{BB}\{\nabla^2(\partial f / \partial c_B) - 2K_{AB}\nabla^2 c_A - 2K_{BB}\nabla^2 c_B\}, \quad (4)$$

where M_{ij} are the effective mobilities; $K_{AA} = K_A + K_C$, $K_{BB} = K_B + K_C$ and $K_{AB} = K_{BA} = K_C$. We have used a characteristic length $l^* = (K_A^*)^{1/2} / 2k_B T$ and a characteristic time, $t^* = (k_B T / M_{AA}^* l^{*2})$ to render the above equations non-dimensional; the superscript * indicates the dimensional quantities. We use a semi-implicit Fourier spectral method (Chen and Shen 1998) for solving (3) and (4), by transforming the partial differential equations into a sequence of ordinary differential equations in Fourier space. Fourier transform of the kinetic equations gives

$$\frac{\partial \tilde{c}_A(\mathbf{k},t)}{\partial t} = M_{AA}\{-k^2(\partial f / \partial c_A)_{\mathbf{k}} - 2K_{AA}k^4\tilde{c}_A - 2K_{AB}k^4\tilde{c}_B\} + M_{AB}\{-k^2(\partial f / \partial c_B)_{\mathbf{k}} - 2K_{AB}k^4\tilde{c}_A - 2K_{BB}k^4\tilde{c}_B\}, \quad (5)$$

$$\frac{\partial \tilde{c}_B(\mathbf{k},t)}{\partial t} = M_{BA}\{-k^2(\partial f / \partial c_A)_{\mathbf{k}} - 2K_{AA}k^4\tilde{c}_A - 2K_{AB}k^4\tilde{c}_B\} + M_{BB}\{-k^2(\partial f / \partial c_B)_{\mathbf{k}} - 2K_{AB}k^4\tilde{c}_A - 2K_{BB}k^4\tilde{c}_B\}, \quad (6)$$

where $\mathbf{k} = (k_x, k_y)$ is the reciprocal lattice vector; $k = |\mathbf{k}|$; $\tilde{c}_A(\mathbf{k},t)$ and $\tilde{c}_B(\mathbf{k},t)$ are the fourier transforms of the respective compositions in the real space. $(\partial f/\partial c_A)_{\mathbf{k}}$ and $(\partial f/\partial c_B)_{\mathbf{k}}$ are the Fourier transforms of the fields, $\partial f/\partial c_A$ and $\partial f/\partial c_B$, respectively. We treat the linear fourth-order terms in (5) and (6) implicitly and the non-linear terms explicitly.

3. Results and discussion

We choose an effective interaction energy parameter (χ) value of 3·5 for our present simulations. With the assumption that the ternary alloy is composed of bulk, homogeneous phases, the isothermal section ($\chi = 3{\cdot}5$) of the phase diagram is drawn schematically in figure 1. In this figure, the A-rich, B-rich and C-rich phases are labeled as α, β and γ, respectively. At $\chi = 3{\cdot}5$ the equilibrium compositions of α, β and γ phases in any alloy in the three-phase field are $(c_A, c_B, c_C) = (0{\cdot}91,\ 0{\cdot}045,\ 0{\cdot}045)$, $(0{\cdot}045,\ 0{\cdot}91,\ 0{\cdot}045)$ and $(0{\cdot}045,\ 0{\cdot}045,\ 0{\cdot}91)$, respectively. In all the simulations, we have used scaled mobilities: $M_{AA} = 1{\cdot}0$, $M_{BB} = 1{\cdot}0$ and $M_{AB} = M_{BA} = -0{\cdot}5$.

The compositions that are chosen for our present study are indicated by the points P and Q along the lines C–d and B–e in figure 1. We choose two sets of values for the gradient energy coefficients, K_A, K_B and K_C and also calculate the corresponding interfacial energies, $\sigma_{\alpha\beta}$, $\sigma_{\alpha\gamma}$ and $\sigma_{\beta\gamma}$ (Huang *et al* 1999). These are given in table 1.

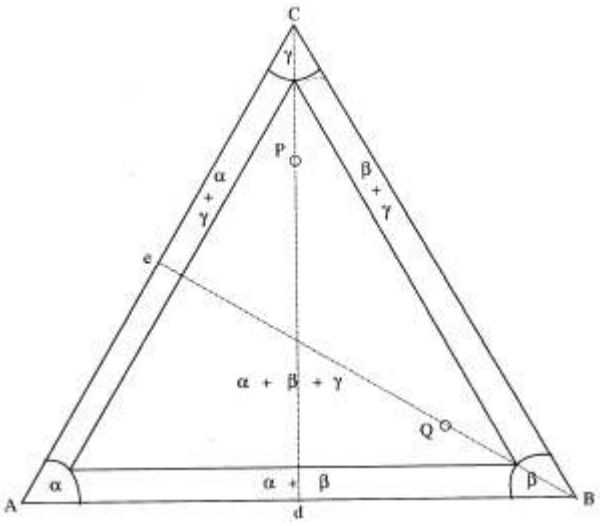

Figure 1. Isothermal section of the phase diagram at $\chi = 3{\cdot}5$ (schematic).

For the first case, the points P and Q in figure 1 are equivalent. Both of them would produce microstructures with identical features. But in the second case, the alloys represented by the points P and Q are distinct with respect to the interfacial properties.

We carry out our simulations on a 256×256 square grid using periodic boundary conditions. The dimensionless time step for integration, δ, is 0·05. Each simulation starts with a prescribed homogeneous composition, with a uniform random fluctuation between –0·005 and +0·005 at each grid point. The results are presented as time snapshots using a gray scale representation of the local concentrations of the species A, B and C. A gray-scale map of the Gibbs triangle (i.e. the concentration triangle) is shown in figure 2.

Case I: $\sigma_{\alpha\beta} = \sigma_{\beta\gamma} = \sigma_{\alpha\gamma}$; $c = c_A = c_B = 0{\cdot}25$; $c_C = 0{\cdot}5$

In this case, the system is represented by the point P in figure 1. The bulk free energy $f(c_A, c_B, c_C)$, has a negative curvature along the line Cd whereas it has a positive curvature along the line AB. Hence the concentration modulation sets up along line Cd since the driving force for spinodal decomposition is along the C–d direction.

So at short times ($t = 300$), the simulated microstructure shows a pseudo-binary phase separation (see figure 3), i.e. the decomposition primarily takes place along the C–d direction producing an interconnected two-phase microstructure consisting of stable 'C-rich' γ phase and an unstable 'C-poor' phase. At a later time, secondary phase separation of C-poor phase into A-rich and B-rich phases results in the formation of discrete, alternating α and β particles. This gives rise to a beaded microstructure, with α and β particles forming the alternate beads. The γ phase is continuous, due to its high volume fraction of about 50%.

Table 1. Gradient energy parameters and sealed interfacial energies.

Case	K_A	K_B	K_C	$\sigma_{\alpha\beta}$	$\sigma_{\alpha\gamma}$	$\sigma_{\beta\gamma}$
I	4·0	4·0	4·0	1·195	1·195	1·195
II	4·0	32·0	4·0	2·628	1·236	2·628

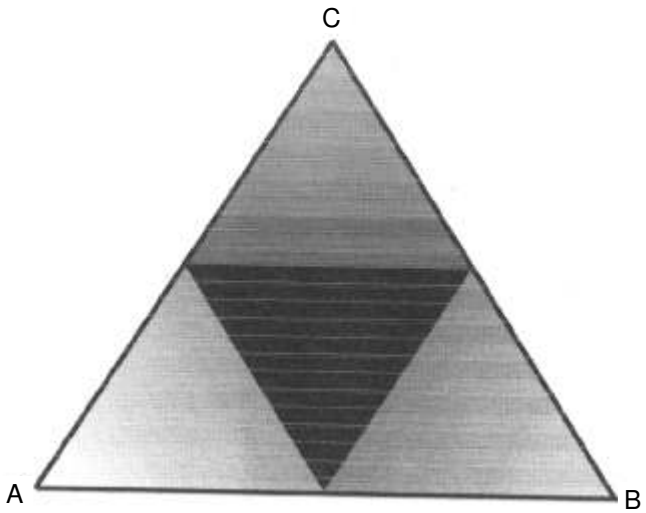

Figure 2. Grayscale colour map projected on Gibbs triangle.

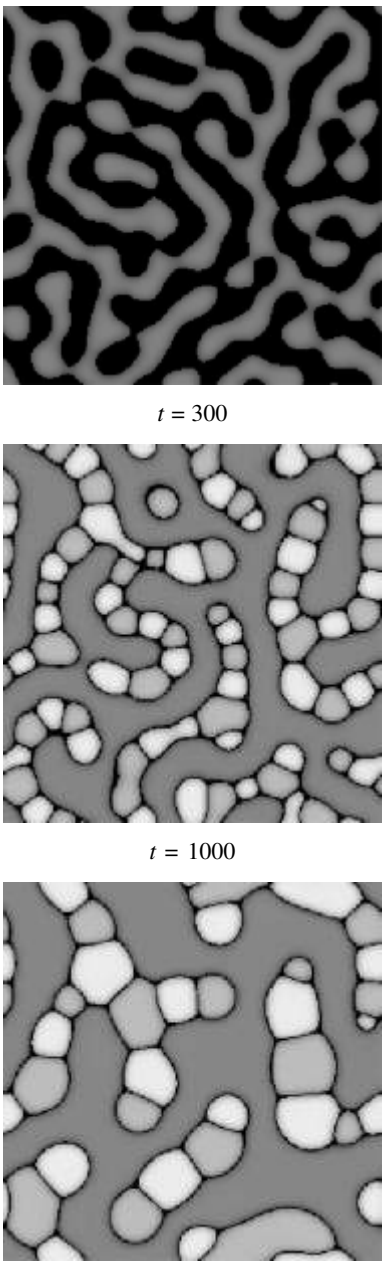

Figure 3. Three-phase separation with $c_A = c_B = 0{\cdot}25$, $c_C = 0{\cdot}5$ and $\sigma_{\alpha\beta} = \sigma_{\beta\gamma} = \sigma_{\alpha\gamma}$.

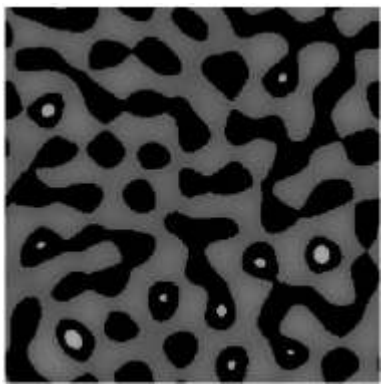

t = 300

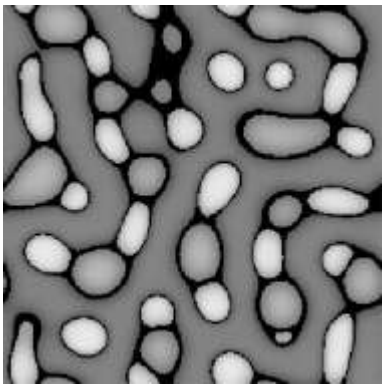

t = 1000

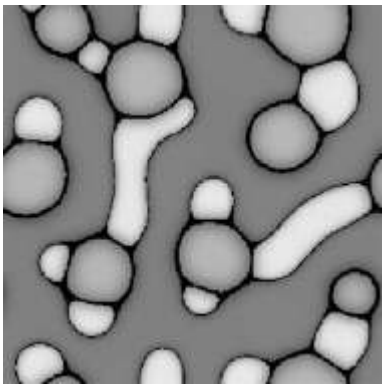

t = 3000

Figure 4. Three-phase separation with $c_A = c_B = 0{\cdot}25$, $c_C = 0{\cdot}5$ and $\sigma_{\alpha\beta} = \sigma_{\beta\gamma} > \sigma_{\alpha\gamma}$.

t = 300

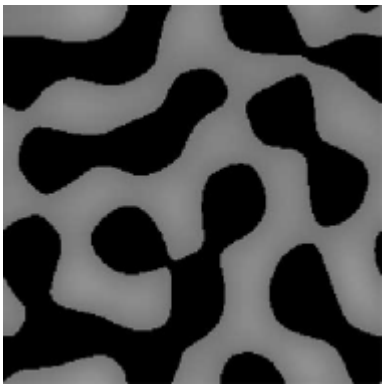

t = 1000

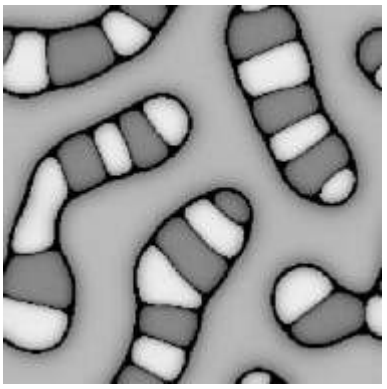

t = 3000

Figure 5. Three-phase separation with $c_A = c_C = 0{\cdot}25$, $c_B = 0{\cdot}5$ and $\sigma_{\alpha\beta} = \sigma_{\beta\gamma} > \sigma_{\alpha\gamma}$.

Case IIa: $\sigma_{\alpha\beta} = \sigma_{\beta\gamma} \sim 2\sigma_{\alpha\gamma}$; $c = c_A = c_B = 0{\cdot}25$; $c_C = 0{\cdot}5$

In this case the interfacial energies of the α–β and the β–γ interfaces are approximately two times that of the α–γ interface. The initial decomposition results in the formation of a C-rich phase and a C-poor phase (see figure 4). But the phases are not interconnected and the C-rich phase has a much higher volume fraction than the C-poor phase (t = 300). The onset of formation of A-rich α phase is observed while formation of B-rich β phase is suppressed due to the higher interfacial energy associated with it. Only at later times (t = 1000) the β phase starts appearing. The β particles are much more rounded than the α particles.

Case IIb: $\sigma_{\alpha\beta} = \sigma_{\beta\gamma} \sim 2\sigma_{\alpha\gamma}$; $c = c_A = c_C = 0{\cdot}25$; $c_B = 0{\cdot}5$

The composition of the alloy is denoted by the point Q in figure 1. In this case, the composition modulations occur along the *B–e* direction. So primary decomposition leads to the formation of stable B-rich β phase and an unstable B-poor phase (see figure 5). If we compare the length scale of this microstructure with the previous two cases, we observe

that the B-rich and B-poor regions are coarser in this case ($t = 300$). The domains remain interconnected before the onset of secondary phase separation of the unstable B-poor phase. At $t = 3000$, the unstable phase decomposes forming alternating beads of α and γ phases. The interconnectivity breaks down at the later stage and we observe discrete beaded structures embedded in a B-rich matrix.

4. Conclusions

In this study, we have shown that the relative interfacial energies between the different phases affect significantly the temporal evolution of microstructure in a ternary alloy system. We observe that the phases associated with a higher interfacial energy appear in the microstructure only at later times. If the chains (produced during secondary phase separation) contain alternating beads having different interfacial energies relative to the matrix, the beads associated with higher interfacial energy are more rounded than those with lower interfacial energy. We also infer qualitatively that the kinetic paths (i.e. the history of the A-rich, B-rich and C-rich phases) are affected significantly by the relative interfacial energies of the three phases.

Acknowledgements

We thank the Department of Science and Technology, New Delhi, for financial support for this work through a research grant.

References

Bhattacharyya S 2002 *Phase separation in ternary alloys: A diffuse interface approach*, M.Sc. (Engg.) Thesis, Department of Metallurgy, Indian Institute of Science, Bangalore (to be submitted)

Cahn J W and Hilliard J E 1958 *J. Chem. Phys.* **28** 258

Chen L Q 1994 *Acta Metall. Mater.* **42** 3503

Chen L Q and Shen J 1998 *Comput. Phys. Commun.* **108** 147

de Fontaine D 1972 *J. Phys. Chem. Solids* **33** 297

de Fontaine D 1973 *J. Phys. Chem. Solids* **34** 1285

Eyre D J 1995 *Mathematics of microstructure evolution* (eds) L Q Chen *et al* (Ohio: TMS-SIAM) p. 367

Hilliard J E 1970 *Phase transformations* (ed.) H I Aaronson (Metals Park, Ohio: ASM)

Hoyt J J 1989 *Acta Metall.* **37** 2489

Hoyt J J 1998 *Acta Mater.* **47** 345

Huang C, Olvera dela Cruz and Swift B W 1995 *Macromolecules* **28** 7996

Huang C, Olvera dela Cruz and Voorhees P W 1999 *Acta Mater.* **17** 4449

Kikuchi R 1997 *Acta Metall.* **25** 195

Kikuchi R, de Fontaine D, Murakami M and Nakamura T 1977 *Acta Metall.* **25** 207

Langer J S 1971 *Ann. Phys.* **65** 53

Langer J S 1973 *Acta Metall.* **21** 1649

Meijering J L 1950 *Philips Res. Rep.* **5** 333

Meijering J L 1951 *Philips Res. Rep.* **6** 183

Morral J E and Cahn J W 1971 *Acta Metall.* **19** 1037